Article

Quantitative Analysis of Catalysis and Inhibition at Horseradish Peroxidase Monolayers Immobilized on an Electrode Surface

Benot Limoges, Jean-Michel Savant, and Dounia Yazidi

J. Am. Chem. Soc., **2003**, 125 (30), 9192-9203• DOI: 10.1021/ja0354263 • Publication Date (Web): 01 July 2003

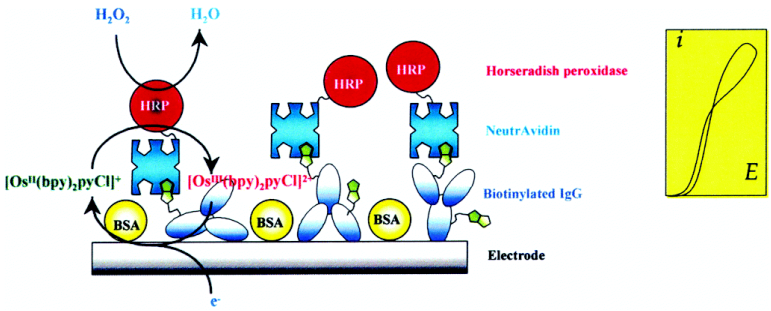

More About This Article

Additional resources and features associated with this article are available within the HTML version:

- Supporting Information
- Links to the 5 articles that cite this article, as of the time of this article download
- Access to high resolution figures
- Links to articles and content related to this article
- Copyright permission to reproduce figures and/or text from this article

View the Full Text HTML

Journal of the American Chemical Society is published by the American Chemical Society. 1155 Sixteenth Street N.W., Washington, DC 20036

J|A|C|S
ARTICLES
Published on Web 07/01/2003

Quantitative Analysis of Catalysis and Inhibition at Horseradish Peroxidase Monolayers Immobilized on an Electrode Surface

Benoît Limoges,* Jean-Michel Savéant,* and Dounia Yazidi

Contribution from the Laboratoire d'Electrochimie Moléculaire de l'Université Denis Diderot (Paris 7), UMR CNRS 7591, 2 place Jussieu, 75251 Paris Cedex 05, France

Received April 2, 2003; E-mail: limoges@paris7.jussieu.fr; saveant@laposte.net

Abstract: Out of several tries, biotinylation of the electrode surface by means of a sacrificial biotinylated immunoglobulin, followed by the anchoring of an avidin-enzyme conjugate appears as the best procedure for depositing a horseradish peroxidase (HRP) monolayer onto an electrode surface, allowing a high-yield immobilization of the enzyme within a stable and highly catalytic coating. Cyclic voltammetry is an efficient means for analyzing the catalytic reduction of H_2O_2 at such HRP monolayer electrodes in the presence of $[Os^{III}(bpy)_2pyCl]^{2+}$ (with bpy = bipyridine and py = pyridine) as a one-electron reversible cosubstrate. The odd shapes of current−potential responses, unusual bell-shaped variation of the peak or plateau current with the substrate concentration, hysteresis and trace crossing phenomena, and dependence or lack of dependence with the scan rate, can all be explained and quantitatively analyzed in the framework of the same catalysis/inhibition mechanism as previously demonstrated for homogeneous systems, taking substrate and cosubstrate mass transport of into account. According to H_2O_2 concentration, limiting-behavior analyses based on the dominant factors or complete numerical simulation were used in the treatment of experimental data. The kinetic characteristics derived from these quantitative treatments implemented by the determination of the amount of enzyme deposited by the newly developed droplet depletion method allowed a comparison with homogeneous characteristics to be drawn. It shows that HRP remains nearly fully active once anchored on the electrode surface through the avidin−biotin linkage. On the basis of this full mechanistic and kinetic characterization, the analytical performances in H_2O_2 detection and amperometric immunosensor applications are finally discussed.

Introduction

The horseradish peroxidase enzyme (HRP) has been involved in numerous applications such as diagnostic assays,[1] nucleic acid analysis,[2] biosensors,[3] bioremediations,[4] polymer synthesis,[5] and other biotechnological processes.[6] Many of these applications take advantage of the immobilization of HRP on a solid support. The methods used for the immobilization of HRP include sol−gel encapsulation,[7] polymer entrapment,[8] physical adsorption (electrostatic[9] and hydrophobic[10] adhesion), covalent attachment,[11,12] and biospecific recognition.[13] In all of these applications, knowing the exact amount of active HRP which

(1) Gosling, J. P. *Clin. Chem.* **1990**, *36*, 1408.
(2) (a) Pollard-Knight, D. *Technique*, **1990**, *2*, 113. (b) Durant, I. *Nonradioact. Labeling Detect. Biomol.* **1992**, 127.
(3) Ruzgas, T.; Csöregi, E.; Emnéus, J.; Gorton, L.; Marko-Varga G. *Anal. Chim. Acta* **1996**, *330*, 123.
(4) (a) Perelta-Zamora, P.; Esposito, E.; Pelegrini, R.; Groto, R.; Reyes, J.; Duran, N. *Environmental Technol.* **1998**, *19*, 55. (b) Wu, Y.; Taylor, K. E.; Biswas, N.; Bewtra, J. K. *Enzyme Microb. Technol* **1998**, *22*, 315. (c) Cooper, V. A.; Nicell, J. A. *Water Res.* **1996**, *30*, 954. (d) Kenji, T.; Shinji, W.; Hiroyasu, I. *Biotechnol. Bioeng.* **1996**, *51*, 126. (e) Klibanov, A. M.; Morris, E. D. *Enzyme Microb. Technol.* **1981**, *3*, 119.
(5) (a) Fukuoka, T.; Tonami, H.; Maruichi, N.; Uyama, H.; Kobayas, S.; Hideyuki, H. *Macromolecules* **2000**, *33*, 9152. (b) Durand, A.; Lalot, T.; Brigodiot, M.; Maréchal, E. *Polymer* **2000**, *41*, 8183.
(6) (a) Colonna, S.; Gaggero, N.; Richelmi, C.; Pasta, P. *TIBITECH*, **1999**, *17*, 163. (b) Bartlett, P. N.; Pletcher, D.; Zeng, J. *J. Electrochem.* **1999**, *146*, 1088.
(7) (a) Yu, J.; Ju, H. *Anal. Chem.* **2002**, *74*, 3579. (b) Wei, Y.; Dong, H.; Xu, J.; Feng, Q. *ChemPhysChem*, **2002**, *9*, 802. (c) Smith, K.; Silvernail, N. J.; Rodgers, K. R.; Elgren, T. E.; Castro, M.; Parker, R. M. *J. Am. Chem. Soc.* **2002**, *124*, 4247. (d) Gao, C.; Liu, X.; Shen, J.; Möhwald, H. *Chem. Commun.* **2002**, 1928. (e) Lloyd, C. R.; Eyring, E. M. *Langmuir*, **2000**, *16*, 9092. (f) Shen, S.; Tu, S. *Biotechnol. Appl. Biochem.* **1999**, *29*, 185.
(8) (a) Gaspar, S.; Habermüller, K.; Csöregi, E.; Schuhmann, W. *Sens. Actuators B* **2001**, *72*, 63. (b) Liu, H.; Ying, T.; Sun, K.; Li, H.; Qi, D. *Anal. Chim. Acta* **1997**, *344*, 187. (c) Lumley-Woodyear, T.; Rocca, P.; Lindsay, J.; Dror, Y.; Freeman, A.; Heller, A. *Anal. Chem.* **1995**, *67*, 1332. (d) Deng. Q.; Dong, S. *J. Electroanal. Chem.* **1994**, *377*, 191. (e) Vreeke, M.; Maidan, R.; Heller, A. *Anal. Chem.* **1992**, *64*, 3084. (f) Tatsuma, T.; Gondaira, M.; Watanabe, T. *Anal. Chem.* **1992**, *64*, 1183.
(9) (a) Caruso, F.; Schuler, C. *Langmuir*, **2000**, *16*, 9595. (b) Rosca, V.; Popescu, I. C. *Electrochem. Commun.* **2002**, *4*, 904. (c) Kirkor, E. S.; Scheeline, A. *J. Phys. Chem. B* **2001**, *105*, 6278.
(10) (a) Ferapontova, E. E.; Grigorenko, V. G.; Egorov, A. M.; Börchers, T.; Ruzgas, T.; Gorton, L. *Biosens. Bioelectron.* **2001**, *16*, 147. (b) Lingren, A.; Ruzgas, T.; Gorton, L.; Csöregi, E.; Ardila, G. B.; Sakharov, I. Y.; Gazaryan, I. G. *Biosensors Bioelectronics*, **2000**, *15*, 491. (c) Lingren, A.; Tanaka, M.; Ruzgas, T.; Gorton, L.; Gazaryan, I. G.; Ishimori, K.; Morishima, I. *Electrochem. Commun.*, **1999**, *1*, 171. (d) Tsai, W.; Cass, A. E. G. *Analyst* **1995**, *120*, 2249. (e) Ruzgas, T.; Emnéus, J.; Gorton, L.; Marko-Varga G. *J. Electroanal. Chem.* **1995**, *391*, 41. (f) Ho, W. O.; Ahtey, D.; McNeil, C. J.; Hager, H. J.; Evans, G. P.; Mullen, W. H. *J. Electroanal. Chem.* **1993**, *351*, 185.
(11) (a) Abad, J. M.; Velez, M.; Santamaria, C.; Guisan, J. M.; Matheus, P. R.; Vazquez, L.; Gazaryan, I.; Gorton, L.; Gibson, T.; Fernandez, V. M. *J. Am. Chem. Soc.* **2002**, *124*, 12 845. (b) Darder, M.; Takada, K.; Pariente, F.; Lorenzo, E.; Abruña, H. D. *Anal. Chem.* **1999**, *71*, 5530. (c) Sun, J.-J.; Fang, H.-Q.; Chen, H.-Y. *Analyst* **1998**, *123*, 1365. (d) Ruan, C.; Yang, F.; Lei, C.; Deng, J. *Anal. Chem.* **1998**, *70*, 1721. (e) Hobara, D.; Uno, Y.; Kakiuchi, T. *Phys. Chem. Chem. Phys.* **2001**, *3*, 3437. (f) Tatsuma, T.; Okawa, Y.; Watanabe, T. *Anal. Chem.* **1989**, *61*, 2352. (g) Smit, M. H.; Cass, A. E. G. *Anal. Chem.* **1990**, *62*, 2429. (h) Bourdillon, C.; Beley, C. *New J. Chem.* **1983**, *7*, 521.

 10.1021/ja0354263 CCC: $25.00

has been immobilized on a solid surface and understanding the key parameters that govern its catalytic activity is a central issue.

Among the various methods available for the determination and the characterization of the activity of immobilized enzymes, electrochemical approaches, such as cyclic voltammetry, involving a redox enzyme on the surface of an electrode and a redox cosubstrate (mediator) that shuttles electrons between the electrode and the prosthetic group of the enzyme, are particularly well suited.[14] The main advantage of cyclic voltammetry is that it gives a simple and rapid overview of the dynamics of mass transfer and kinetics occurring at the electrode surface. Many procedures have been proposed to immobilized the HRP onto electrode surfaces[3,7a,8,10,11,13b,c,e−g] and some efforts made to determine the coverage of HRP monolayers.[10a,d,11a,b,f,12b,13b] However, the nature and characteristics of the mechanism, the respective role of enzyme kinetics and mass transport of the substrate (H_2O_2) and cosubstrate (electron donor) and the precise determination of the amount of HRP that remains active once immobilized are largely unsettled issues. One of the major difficulties in reaching these goals lies in the complexity of the mechanism of catalysis and inhibition involved in the reaction of HRP with its H_2O_2 substrate. This complex mechanism has been established recently in the case where the enzyme is homogeneously dispersed in the solution, through a systematic cyclic voltammetric analysis of the mediated electrochemistry of HRP in the presence of different concentrations of the substrate and cosubstrate.[15] Another crucial issue is the design of an immobilization method leading to a stable and well-defined (and/or spatially controlled) deposition of the enzyme onto the electrode surface, minimizing the loss of its catalytic function through a partial denaturation, steric hindrance, or conformational changes.

Among the large variety of immobilization strategies, chemical attachment leading to the formation of irreversible covalent bonds between amino acids or carbohydrates residues in HRP and reactive groups on the support is one of the most widely investigated.[11,12] However, the formation of saturated monolayer of HRP requires the use of relatively high concentrations of enzyme in solution during the coupling step, leading to significant nonspecific adsorption of the enzyme triggering the formation of aggregates of probably denatured protein.[11a,12b] These drawbacks can be avoided using a bioaffinity-based enzyme immobilization,[16] in which much lower concentrations of enzyme are required. Moreover, such an immobilization procedure can result in enzyme preparations that exhibit a fully preserved catalytic activity and an improved stability against denaturation. This has been shown in the case of monolayer, as well as multilayers, of glucose oxidase specifically attached on an electrode surface with an antigen−antibody interaction.[14c−e] It has been also observed for a biomolecular assemblage based on a biotin−avidin recognition.[14a,b]

Another interesting facet of the bioaffinity immobilization of HRP onto electrode surfaces is its application as a sensitive catalytic label in electrochemical immunosensors.[17] In these systems, the specific molecular recognition between an antigen and an antibody assembled on the electrode, is converted into an electrochemical signal by means of the electrocatalytic activity of the HRP attached to the immunocomplex. This field was recently extended to the detection of nucleic acid hybrids with the help of an HRP-labeled oligonucleotide probe.[18] It is important to note that in most of theses applications, direct electron transfer between the redox enzyme and the electrode is precluded by steric hindrance. A mediator serving as artificial cosubstrate is thus required to shuttle the electrons between the electrode and the enzyme.

The construction of a stable and well-organized monolayer of HRP on the surface of a carbon electrode depicted below takes advantage of the strong affinity of biotin for the four noncooperative binding sites of avidin. The enzyme electrodes thus prepared are then investigated by means of cyclic voltammetry, so as to fully characterize their activity and the catalysis kinetics in the presence of the natural substrate, H_2O_2, and of the reversible cosubstrate couple, $[Os(bpy)_2pyCl]^{2+}/[Os(bpy)_2pyCl]^{+}$. The main task of the work described below was to understand the behavior of HRP once immobilized on an electrode surface so as to provide sound guidelines for the development of HRP-linked detection strategies. To discuss this issue, we will start from the mechanism established previously in the homogeneous case,[15] which involves the reaction scheme recalled below (Scheme 1). P and Q are the oxidized ($[Os^{III}(bpy)_2pyCl]^{2+}$) and reduced ($[Os^{II}(bpy)_2pyCl]^{+}$) forms of the mediator, respectively, S, the H_2O_2 substrate, E, the native ferriperoxidase (Fe^{III}), E_1, the oxyferryl π-cation radical compound I ($[Fe^{IV}=O]^{\bullet+}$), E_2, the oxyferryl compound II ($Fe^{IV}=O$), E_3, the oxyperoxidase ($Fe^{II}-O_2$), and ES, E_1Q, and E_2Q, the precursor complexes that may be formed with the reactive form of substrate and cosubstrate.

We will first describe the immobilization method we selected after comparison with other possible approaches. A preliminary investigation of key cyclic voltammetric responses will then allow us to assess the stability of these electrodes. After a brief qualitative assessment of the reaction mechanism, we will present a quantitative analysis of the kinetics of catalysis and

(12) (a) Avezedo, A. M.; Prazeres, D. M. F.; Cabral, J. M. S.; Fonseca, L. P. *J. Mol. Catal. B: Enzymol.* **2001**, *15*, 147. (b) Vianello, F.; Zennaro, L.; Di Paolo, M. L.; Rigo, A.; Malacarne, C.; Scarpa, M. *Biotechnol. Bioeng.* **2000**, *68*, 488. (c) Pundir, C. S.; Malik, V.; Bhargava, A. K.; Thakur, M.; Kalia, V.; Singh, S.; Kuchhal, N. K. *J. Plant Biochem. Biotechnol.* **1999**, *8*, 123. (d) Husain, S.; Jafri, F.; Saleemuddin, M. *Biochem. Mol. Biol. Int.* **1996**, *40*, 1. (e) Yan, M.; Cai, S. X.; Wybourne, M. N.; Keana, J. F. W. *J. Am. Chem. Soc.* **1993**, *115*, 814.

(13) (a) Fishman, A.; Ley, I.; Cogan, U.; Shoseyov, O. *J. Mol. Catal. B: Enzymol.* **2002**, *18*, 121. (b) Kobayashi, Y.; Anzai, J. *J. Electroanal. Chem.* **2001**, *507*, 250. (c) Karyakin, A. A.; Presnova, G. V.; Rubtsova, M. Y.; Egorov, A. M. *Anal. Chem.* **2000**, *72*, 3805. (d) Rao, S. V.; Anderson, K. W.; Bachas, L. G. *Biotechnol. Bioeng.* **1999**, *65*, 389. (e) Vreeke, M.; Rocca, P.; Heller, A. *Anal. Chem.* **1995**, *67*, 303. (f) Lu, B.; Iwuoha, E. I.; Smyth, M. R.; O'Kennedy, R. *Anal. Commun.* **1997**, *34*, 21. (g) Pantano, P.; Hellman, M.; Kuhr, W. G. *J. Am. Chem. Soc.* **1991**, *13*, 1832.

(14) (a) Anicet, A.; Anne, A.; Moiroux, J.; Savéant, J.-M. *J. Am. Chem. Soc.* **1998**, *120*, 7115. (b) Anicet, N.; Bourdillon, C.; Moiroux, J.; Savéant, J−M. *J. Phys. Chem. B* **1998**, *102*, 9844. (c) Bourdillon, C.; Demaille, C.; Moiroux, J.; Savéant, J−M. *J. Am. Chem. Soc.* **1995**, *117*, 11 499. (d) Bourdillon, C.; Demaille, C.; Moiroux, J.; Savéant, J−M. *J. Am. Chem. Soc.* **1994**, *116*, 10 328. (e) Bourdillon, C.; Demaille, C.; Gueris, C.; Moiroux, J.; Savéant, J.-M. *J. Am. Chem. Soc.* **1993**, *115*, 12 264.

(15) Dequaire, M.; Limoges, B.; Moiroux, J.; Savéant, J.-M. *J. Am. Chem. Soc.* **2002**, *124*, 240.

(16) Saleemuddin, M. *Adv. Biochem. Eng. Biotechnol*. **1999**, *64*, 203.

(17) (a) Kasai, S.; Yokota, A.; Zhou, H.; Nishizawa, M.; Niwa, K.; Onouchi, T.; Matsue, T. *Anal. Chem.* **2000**, *72*, 5761. (b) Campbell, C. N.; Lumley-Woodyear, T.; Heller, A. *Fresenius J. Anal. Chem.* **1999**, *364*, 165. (c) Del Carlo, M.; Mascini, M. *Anal. Chim. Acta* **1996**, *336*, 167. (d) Pritchard, D. J.; Morgan, H.; Cooper, J. M. *Anal. Chim. Acta* **1995**, *310*, 251. (e) Kalab, T.; Skladal P. *Anal. Chim. Acta* **1995**, *304*, 361. (f) Deasy, B.; Dempsey, E.; Smyth, M. R.; Egan, D.; Bogan, D.; O'Kennedy, R. *Anal. Chim. Acta* **1994**, *294*, 291. (g) O'Daly, J. P.; Zhao, J.; Brown, P. A.; Henkens, R. W. *Enzyme Microb. Technol*. **1992**, *14*, 299.

(18) (a) Dequaire, M.; Heller, A. *Anal. Chem.* **2002**, *74*, 4370. (b) Campbell, C. N.; Gal, D.; Cristler, N.; Banditrat, C.; Heller, A. *Anal. Chem.* **2002**, *74*, 158. (c) Azek, F.; Grossiord, C.; Joannes, M.; Limoges, B.; Brossier, P. *Anal. Biochem.* **2000**, *284*, 107. (d) Caruana, D. J.; Heller, A. *J. Am. Chem. Soc.* **1999**, *121*, 769. (e) Lumley-Woodyear, T.; Caruana, D. J.; Campbell, C. N.; Heller, A. *Anal. Chem.* **1999**, *71*, 394.

Scheme 1

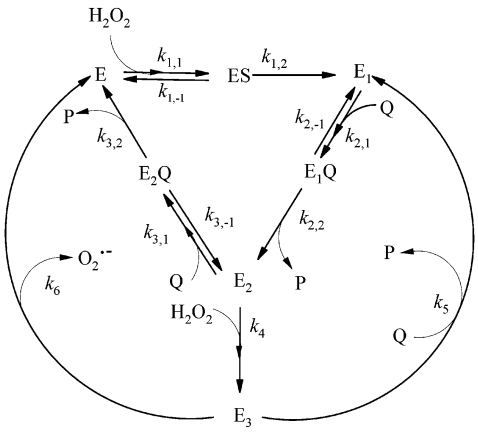

inhibition. It allows the determination of the individual rate constants of the two inhibition/recovery loops, but, concerning the main catalytic loop, only of the product of the rate constant k_3 ($k_3 = k_{3,1}k_{3,2}/(k_{3,-1} + k_{3,2})$) by the surface concentration of enzyme. Independent methods for reaching the surface concentration of enzyme will thus be described, allowing an estimation of the enzyme activity after immobilization. We will close with a short note discussing the analytical sensitivity of the enzyme electrode.

The Supporting Information section provides the demonstration of the kinetic equations used in the article and of the numerical computation procedures.

Results and Discussion

Immobilization of the Enzyme on the Electrode. The procedure we used for the immobilization of HRP is outlined in Figure 1. A saturated monolayer of biotinylated rabbit IgG (IgG-b) was first irreversibly adsorbed on the surface of the carbon electrode, followed by saturation of the unoccupied sites with bovine serum albumin (BSA). The neutravidin-HRP conjugate (N−HRP) was then specifically attached, thanks to its strong affinity for the biotin moieties. The neutravidin protein coupled to HRP is a deglycosylated form of avidin that offers the advantage of a neutral isoelelectric point (pI = 6.3), thus minimizing nonspecific absorption. Unless otherwise stated, screen-printed electrodes (SPEs) obtained from a graphite/polystyrene ink have been used all along this work owing to their low background current, good reproducibility and convenient handling. The SPEs have the further advantage of being particularly well adapted for the mass production of low-cost disposable biosensors.[19] The $[Os^{III}(bpy)_2pyCl]^{2+}$ was selected as the free diffusing reversible one-electron mediator. It is the same as previously used to characterize the mechanism and kinetics of the catalysis and inhibition of the oxidation of H_2O_2 by dissolved HRP.[15]

The above immobilization procedure was selected after investigation of other approaches. In these preliminary experiments, we tested the direct adsorption of native HRP on the SPE. The amount of deposited active enzyme was estimated from the voltammetric response of the electrode after addition of H_2O_2 and P, in the solution. When a significant amount of active enzyme is deposited on the electrode, a catalytic wave is observed and the surface concentration of active enzyme, Γ^0, may be derived from the catalytic current, as it will be shown latter on. The catalytic currents obtained at SPEs immersed for 2 h in 0.2 μM of HRP were very low, indicating a value of Γ^0 ranging from 0.1 to 0.4 pmol cm^{-2}. Reproducibility was poor. Moreover, the catalytic response was continuously declining upon repetitive use and storage of the electrode. These results are consistent with a weak adsorption of the native enzyme on the hydrophobic surface of the carbon-based electrode. This is not surprising because HRP is highly glycosylated and thus hydrophilic. We have found, however, that, under similar conditions, the direct adsorption of the more hydrophobic N−HRP conjugate leads to appreciable catalytic currents, with an estimated value of $\Gamma^0 \sim 1$ pmol cm^{-2}. In agreement with the stronger adsorption of the conjugate, the stability of the current response was also observed to be much more stable than with the native enzyme, with a decay of only 15−20% after 60 days of storage at 4 °C in pH 7.4. Although the stability and sensitivity were reasonable, they were not as good as in the case of the specific HRP immobilization through the strong avidin−biotin binding (vide infra). Furthermore, micromolar concentrations of N−HRP in solution were required to saturate the electrode surface by a monolayer of active enzyme after 2 h of incubation time, which is much higher than in the case of the IgG-b/N−HRP assemblage, where submicromolar concentrations sufficed. At such low concentrations, there is less probability of enzyme aggregation on the electrode surface. For these reasons, we have selected the above bioaffinity assemblage and prepared the electrodes by immersion in 0.2 μM of N−HRP during 2 h.

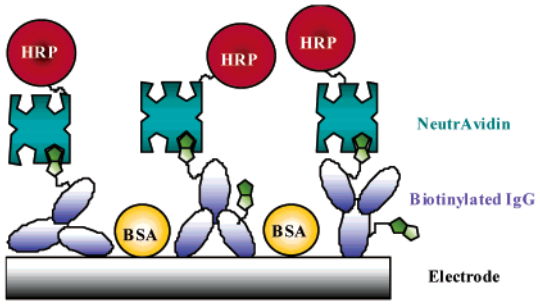

Figure 1. Outline of the monolayer assemblage of HRP on the electrode surface.

Because the HRP used in this work is covalently conjugated to neutravidin, its activity might be somewhat different from the native enzyme. We have then determined the activity of N−HRP, as previously,[15] by means of steady-state spectrophotometry in homogeneous solution (see the Experimental Section), and the kinetic rate constants of the rate determining step in the primary catalytic cycle (reaction 3 in Scheme 1) were found to be $k_3 = k_{3,3}/K_{3,M} = (7.85 \pm 1.20) \times 10^6$ M^{-1} s^{-1} and $k_{3,2} = 200 \pm 80$ s^{-1}, thus leading to a Michaelis constant of $K_{3,M} = 25 \pm 10$ μM. This latter value is in good agreement with that previously obtained for the native enzyme,[15] whereas the constant k_3 is ~10−20% lower, suggesting that the HRP moiety in the conjugate is ~80−90% active.

(19) Disposable glucose electrode based on disposable screen-printed enzyme electrodes are the basis of the majority of commercialized personal blood glucose meters. (a) Matthews, D. R.; Holman, R. R.; Bown, E.; Steemson, J.; Watson, A.; Hughes, S.; Scott, D. *Lancet* **1987**, 778. (b) Harn-Shen, C.; Benjamin, K. I.; Chii-Min, H.; Kuang-Chung, S.; Ching Fai, K.; Low-Tone, H. *Diabetes Res. Clin. Pract.* **1998**, *42*, 9. (c) Lehmann, R.; Kayrooz, S.; Greuter, H.; Spinas, G. A. *Diabetes Res. Clin. Pract.* **2001**, *53*, 121.

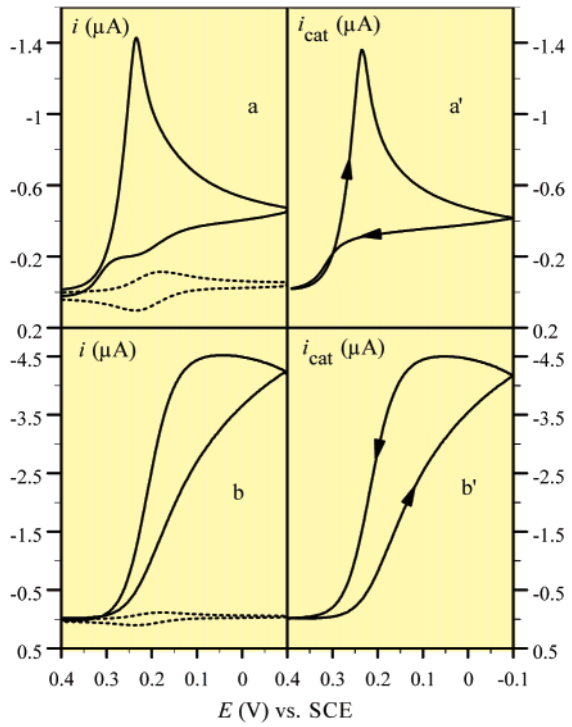

Figure 2. Solid curves represent the cyclic voltammograms recorded at a SPE coated with a monolayer of IgG-b/N−HRP and immersed in a phosphate buffer of pH 7.4, containing 20 μM $[Os(bpy)_2pyCl]^{2+}$ and (a, a′) 0.1 or (b, b′) 1 mM H_2O_2. The dashed curves correspond to the cyclic voltammograms recorded in the absence of H_2O_2. The voltammetric curves shown in a′ and b′ result from the subtraction of the plain curves in a and b to the corresponding dashed curves. Scan rate: 10 mV s^{-1}. Temperature: 20 °C.

Cyclic Voltammetric Responses and Stability. Figure 2 shows a typical set of voltammograms recorded at a SPE coated with a monolayer of IgG-b which was beforehand immersed for 2 h in a solution containing 0.2 μM N−HRP. At a low concentration of H_2O_2 (Figure 2a), the reversible wave of the mediator (dashed line) is converted into an enhanced irreversible wave (plain curve), having a sharp peak shifted in the negative potential direction toward the standard potential of the mediator ($E^0_{P/Q} = 0.21$ V vs SCE). Such behavior is characteristic of an efficient catalysis and of strong substrate consumption in the diffusion layer, leading to the kinetic control of the current by substrate diffusion.[20] When the concentration of H_2O_2 is increased, the peak-shaped current is changed into a plateau-shaped wave, which includes a striking hysteresis effect with a catalytic current during the forward scan being lower to the one obtained throughout the reverse scan (Figure 2b). The tendency to reach a plateau current indicates that the concentration of the substrate is high enough for its concentration in the surface coating to equal its bulk concentration, leading thus to the control of the catalytic current by the enzymatic reaction, whereas the hysteresis effect echoes the slowness of the inactivation/reactivation of the immobilized enzyme, as shown earlier in homogeneous solution.[15] Persistence of some hysteresis at low H_2O_2 concentration is attested by the small curve crossing in the foot of the wave in Figure 2a′. It appears after subtracting from the total current the diffusion-controlled nernstian wave of the cosubstrate obtained when no substrate is present in the solution, as sketched in Figure 2. As seen later on, the current response is indeed the sum of the cosubstrate diffusion current and the catalytic current. In the absence of mediator, no electrocatalytic activity is observed, showing that the direct electron transfer between the prosthetic group of the enzyme, and the electrode surface is ineffective.[21] In the absence of H_2O_2, the osmium mediator gives rise, in the scan rate range of interest, to a fast one-electron reversible cyclic voltammetric wave since the cathodic peak current remains proportional to the square root of the scan rate (υ) up to 1 V s^{-1} and the anodic-to-cathodic peak potential remains close to 60 mV up to 1 V s^{-1}. The presence of the protein layer on the electrode entails a slight decrease of the cathodic and anodic peak currents.

Stability of the electrode response upon storage and repetitive use is a prerequisite for a precise quantitative study of the complex dynamic of immobilized HRP. Stability upon storage at 4 °C in a phosphate buffer of pH 7.4 (PB), gauged by following the cyclic voltammetric responses, was found to be remarkably good, of the order of 5−10% decay of the catalytic response after 60 days of storage and occasional running. Stability is definitely better than observed for monolayers of HRP immobilized by covalent binding (half-life ranging from 10 to 40 days).[11c,f,h,12b] The electrode response during its repetitive use was also observed to be quite stable even in solutions containing high concentrations of H_2O_2. For example, in the solution containing 2 mM of H_2O_2 and 20 μM of P, the catalytic response decreases linearly by 0.24% per min of immersion time. The decay rate does not exceed 0.41%/min in the presence of 20 mM H_2O_2. A similar drop of the catalytic activity of HRP in the presence of a large excess of H_2O_2 has already been observed in homogeneous solutions and ascribed to an irreversible deactivation of the enzyme by H_2O_2 yielding a verdohemoprotein derivative, also designated as P670.[22] This irreversible inactivation pathway of immobilized HRP is a slow process under our experimental conditions and can be considered as negligible when low H_2O_2 concentrations and/or reasonable immersion times are dealt with.

Qualitative Assessment of the Reaction Mechanism. We now set out for a more precise analysis of catalysis and inhibition in these systems, based on the variations of the cyclic voltammetric responses as a function of the substrate concentration. Figure 3 shows a series of voltammetric curves recorded at a same IgG-b-modified electrode coated with a saturated layer of N−HRP and in a large range of H_2O_2 concentrations. Starting from low H_2O_2 concentrations, the catalytic wave exhibits a very sharp peak, with some curve crossing at the foot of the wave.

Upon raising the substrate concentration, the catalytic peak current increases while the sharp peak is progressively converted into an S-shaped wave with growing appearance of curve

(20) Limoges, B.; Moiroux, J.; Savéant, J.-M. *J. Electroanal. Chem.* **2002**, *521*, 8.

(21) The lack of direct electrical contact can be explained by the presence of the first layer of biotinylated protein which remove the enzyme far from the electrode surface. To test for possible catalysis of HRP in a more intimate contact with the electrode, the enzyme was directly adsorbed on a naked SPE or HOPG electrode (immersion in a 0.5 mg $ml^{-1}$of HRP for 2 h), and the voltammogram was recorded in the presence of H_2O_2 (0.6 mM in PB). Comparison of the voltammetric curve with that of an electrode that was not immersed in the HRP solution showed however no measurable difference. This is in contradiction with several published results.[10a−c,e,f]

(22) (a) Hernandez-Ruiz, J.; Arnao, M. B.; Garcia-Canovas, F.; Acosta, M. *Biochem. J.* **2001**, *354*, 107. (b) Rodriguez-Lopez, J. N.; Hernandez-Ruiz, J.; Garcia-Canovas, F.; Thorneley, R. N. F.; Acosta, M.; Arnao, M. B. *J. Biol. Chem.* **1997**, *272*, 5469. (c) Arnao, M. B.; Acosta, M.; del Rio, J.-A.; Varon, R.; Garcia-Canovas, F. *Biochim. Biophys. Acta* **1990**, *1041*, 43. (d) Nakajima, R.; Yamazaki, I. *J. Biol. Chem.* **1980**, *255*, 2067.

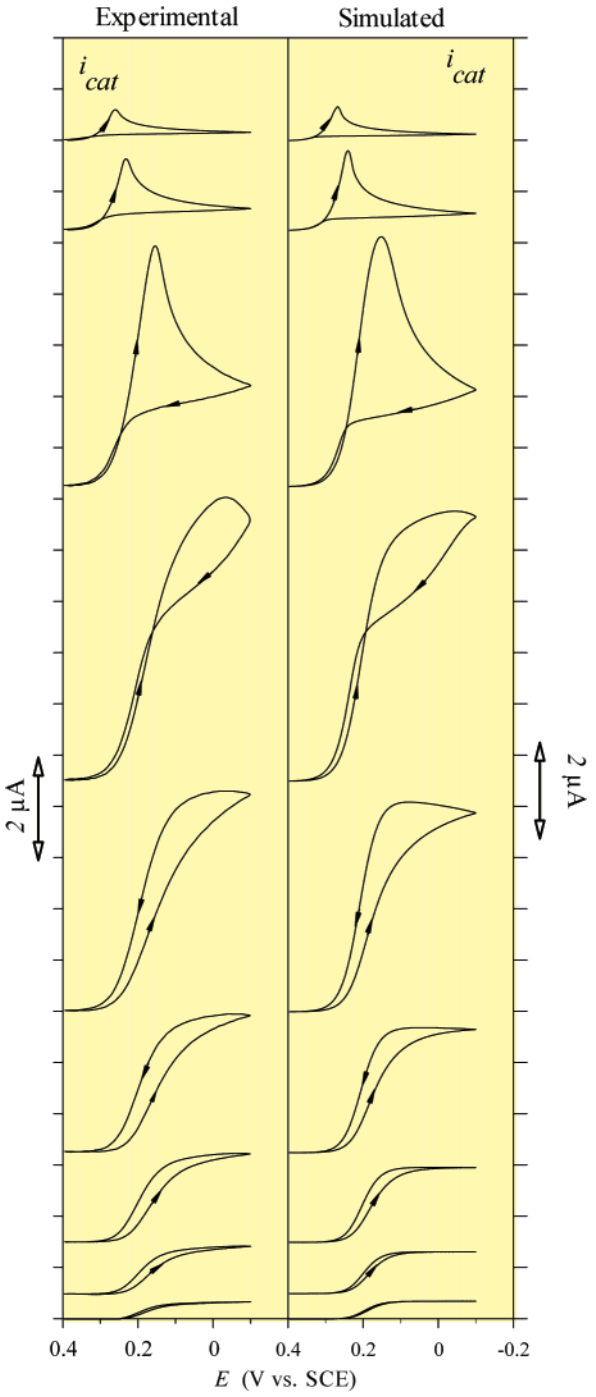

Figure 3. Cyclic voltammograms recorded at a SPE coated by a monolayer of N−HRP and immersed in PB, containing 20 μM $[Os(bpy)_2pyCl]^{2+}$ and increasing concentrations of H_2O_2, from top to bottom: 0.02, 0.05, 0.25, 0.5, 2, 5, 10, 20, 50 mM. Scan rate: 10 mV s^{-1}. Temp: 20 °C. The voltammetric curves are all corrected by subtraction of the reversible wave of the mediator recorded in the absence of H_2O_2 in the same solution. Simulations (see text) were performed using the following values of the parameters: 3.7 pmol cm^{-2}, $k_3\Gamma^0 = 0.029$ cm s^{-1}, $K_{3,M} = 37$ μM, $k_4 = 30$ M^{-1} s^{-1}, $k_5 = 2080$ M^{-1} s^{-1}, $k_6 = 0.01$ s^{-1}, $k_1 = 1.7 \times 10^7$ M^{-1} s^{-1}, $K_{1,M} = 128$ μM, $D_S = 1.5 \times 10^{-5}$ cm^2 s^{-1}.

crossing at the foot of the wave. Upon further increase of the H_2O_2 concentration, the catalytic current gradually decreases, indicating the progressive formation of the inactivated form of HRP, similarly to what was observed with the enzyme in homogeneous solution.[15] At intermediate H_2O_2 concentrations, a significant hysteresis effect appears. Hysteresis decreases at

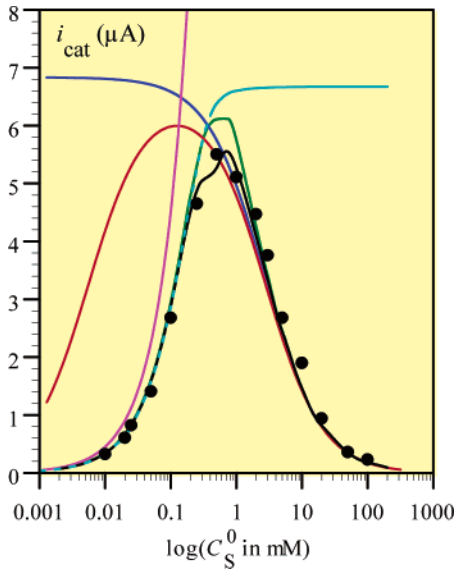

Figure 4. Variation of the voltammetric peak or plateau current with the concentration of H_2O_2 obtained in the same conditions as in Figure 3 (some of the corresponding cyclic voltammetric curves are shown in Figure 3). Solid circles: experimental values. Steady-state equations: application of eq 14 (blue curve), eq 13 (red curve), of a combination of eqs 17 and 18 (cyan curve), of eq 19 (magenta curve), of a combination of eqs 12 and 17 (green curve), with: $k_3\Gamma^0 = 0.029$ cm s^{-1}, $K_{3,M} = 37$ μM, $k_4/k_5 = 0.0144$, $k_6/k_5 = 4.8$ μM, $k_1 = 1.7 \times 10^7$ M^{-1} s^{-1}, $K_{1,M} = 128$ μM, $D_S = 1.5 \times 10^{-5}$ cm^2 s^{-1}. Simulation after removal of the steady-state approximation (black curve): same values of the preceding parameter plus $k_4 = 30$ M^{-1} s^{-1}.

higher substrate concentrations, whereas the wave becomes S-shaped with superimposition of the forward and reverse traces. The upward and then downward variation of the catalytic peak or plateau current with the concentration of H_2O_2 is recapped in Figure 4 from the experiments shown in Figure 3 and others carried out at other H_2O_2 concentrations.

In a first stage, we examine how these observations may receive a qualitative explanation in the framework of the mechanism depicted in Scheme 1. At low H_2O_2 concentrations, inhibition does not interfere significantly. Catalysis is consequently very effective and, because the concentration of H_2O_2 is small, it is consumed to a large extent in the enzyme coating. This is the reason that a sharp peak is observed as a result of partial or total control of the current by substrate diffusion. Upon increasing $[H_2O_2]$, the progressive conversion of the peak-shaped to a plateau-shaped response is indicative of the passage from control by substrate transport to control by the kinetics of the enzymatic reaction. Simultaneously, inhibition according to reaction 4 starts to interfere resulting in the observed decrease of the current. The voltammetric curves were all recorded 5−10 min after the enzyme electrode was immersed into the solution containing the reactants at selected concentrations, so as to ensure, as done previously with the enzyme in homogeneous solution,[15] that a steady-state between the activated and inactivated forms of the enzyme is established before starting the potential scan. Inhibition occurs immediately after immersion of the enzyme electrode (under open circuit) in the H_2O_2-containing solution and a steady-state distribution is reached. This is attained in less than 5 min with, e.g., 0.5 mM H_2O_2. In the absence of a reducing cosubstrate, H_2O_2 is believed to act as a reductant in a slow transformation of E_1 into E_2,[22a] thus opening a route to the conversion of E_2 into E_3, the inactivated

form of HRP (Scheme 1). Once the steady-state distribution is reached at the start of the cyclic voltammogram, the steady-state initial surface concentration of E_3, resulting from the competition between the formation (reaction 4) and decomposition (reaction 6) of the inactivated form of HRP, can be estimated from eq 1

$$\Gamma_{E_3} = \Gamma^0\left(1 - \frac{k_6}{k_4 C_S^0 + k_6}\right) \quad (1)$$

(Γ^0 is the total surface concentration of enzyme on the electrode. The $\Gamma_{\text{subscript}}$ are the surface concentrations of the subscript enzyme form. C_S^0 is the bulk concentration of substrate).

We have previously observed with the soluble enzyme that inhibition of the catalytic current by H_2O_2 is a reversible process, the active enzyme being restored only by reaction 6 in the absence of a reducing cosubstrate (i.e., under open circuit), and by reactions 5 and 6 during the electrocatalytic process. Inhibition is also reversible with the immobilized enzyme since, after the electrode was immersed in solutions containing successively a low and a large H_2O_2 concentration and then rinsed and re-immersed in the starting solution, the catalytic signal was entirely recovered. Restoration of the active enzyme through reaction 5 is the cause that there is still a catalytic response at high H_2O_2 concentrations. It is also the cause of the hysteresis phenomenon, which results from the kinetics of reactions 4 and 5 falling within the time-scale of the potential scan.

Quantitative Analysis of the Kinetics of Catalysis and Inhibition. For one monolayer of HRP immobilized on the electrode, the current flowing through the electrode is given by eq 2 in the framework of Scheme 1, assuming, as always, that diffusion is linear

$$\frac{i}{FS} = -D\left(\frac{\partial[Q]}{\partial x}\right)_{x=0} + k_{3,1}[Q]_{x=0}\Gamma_{E_2} - k_{3,-1}\Gamma_{E_2Q} + k_{2,1}[Q]_{x=0}\Gamma_{E_1} - k_{2,-1}\Gamma_{E_1Q} + k_5[Q]_{x=0}\Gamma_{E_3} \quad (2)$$

where i is the current, F the Faraday constant, S is the electrode area, D the diffusion coefficient of P (assumed to be the same as Q), x the distance from the electrode surface. The subscript $x = 0$ stands for the electrode surface. At time $t = 0$, the concentrations of P and Q are equal throughout the solution to the bulk concentration of P (C_P^0) and to 0, respectively. At the electrode surface, $x = 0$, the reduction of P into Q is governed by the Nernst law and the concentration of Q is given by eq 3 under the assumption that the steady-state approximation applies for all the Michaelis−Menten complexes, ES, E_1Q, E_2Q, and also for E_1, because the conversion of E_1 into E_2 is known to be rapid as compared to the conversion of E_2 to E (see the Supporting Information, which provides also mathematical details for the establishment of the various equations below)

$$[Q]_{x=0} = \frac{C_P^0}{1 + \exp\left[\frac{F}{RT}(E - E_{P/Q}^0)\right]} \quad (3)$$

The current may thus be split into a diffusion contribution, i_{dif}, and a catalytic contribution, i_{cat}

$$\frac{i_{dif}}{FS} = -D\left(\frac{\partial[Q]}{\partial x}\right)_{x=0}$$

$$\frac{i_{cat}}{FS} = k_{3,1}[Q]_{x=0}\Gamma_{E_2} - k_{3,-1}\Gamma_{E_2Q} + k_{2,1}[Q]_{x=0}\Gamma_{E_1} - k_{2,-1}\Gamma_{E_1Q} + k_5[Q]_{x=0}\Gamma_{E_3} \quad (4)$$

The first of these contributions is the nernstian reversible current potential curve that is obtained when no substrate is present. It is given by eq 5 (see the Supporting Information)

$$\frac{1}{\sqrt{\pi}}\int_0^t \frac{i_{dif}}{FS\sqrt{D}\sqrt{Fv/RT}C_P^0}\frac{d\eta}{\sqrt{t-\eta}} = \frac{1}{1 + \exp\left[\frac{F}{RT}(E - E_{P/Q}^0)\right]} \quad (5)$$

with:

during the forward scan: $0 \le t \le t_r$: $E = E_i - vt$

and during the reverse scan: $t_r \le t \le 2t_r$: $E = E_f + v(t - t_r) = 2E_f - E_i + vt$

(E_i: initial potential, E_f: final potential, E_r: potential at scan reversal, t_r: time at scan reversal, v: scan rate). Equation 5 with its two accompanying conditions exactly represents the reversible nernstian diffusion controlled wave of the cosubstrate in the absence of substrate. This is the reason that the nernstian reversible response of the cosubstrate, for the same scan rate, has been systematically subtracted from the total current in order to obtain the catalytic contribution in Figures 2−4 and in the figures to come.

In the most general case, all enzyme forms do not obey the steady-state approximation. We may however deem that, as in the homogeneous case, the approximation applies to the Michaelis−Menten complexes, ES, E_1Q, and E_2Q, as well as to E_1, because reaction 2 is much faster than reaction 3. Equation 4 thus becomes

$$\frac{i_{cat}}{FS} = k_3[Q]_{x=0}\Gamma_{E_2} + k_1[S]_{x=0}\Gamma_E + 2k_5[Q]_{x=0}\Gamma_{E_3} \quad (6)$$

($k_1 = k_{1,1}k_{1,2}/(k_{1,-1} + k_{1,2})$), expression that is further simplified by removing the negligible last term (the role of reaction 5 being more of a reactivation of the catalysis than of a direct contribution to the catalytic current)

$$\frac{i_{cat}}{FS} \cong k_3[Q]_{x=0}\Gamma_{E_2} + k_1[S]_{x=0}\Gamma_E \quad (7)$$

The time-dependent surface concentrations of the three enzyme forms obey the following differential equations (see the Supporting Information)

$$\frac{d\Gamma_{E_2}}{dt} = \frac{\{(-(k_3[Q]_{x=0} + k_4[S]_{x=0})\Gamma_{E_2} + k_1[S]_{x=0}\Gamma_E + k_5[Q]_{x=0}\Gamma_{E_3})\}}{1 + \frac{[Q]_{x=0}}{K_{3,M}}} \quad (8)$$

$$\frac{d\Gamma_E}{dt} = \frac{k_3[Q]_{x=0}\Gamma_{E_2} - k_1[S]_{x=0}\Gamma_E + k_6\Gamma_{E_3}}{1 + \frac{[S]_{x=0}}{K_{1,M}}} \quad (9)$$

$$\left(K_{3\text{ or }1,M} = \frac{k_{3\text{ or }1,-1} + k_{3\text{ or }1,2}}{k_{3\text{ or }1,1}}\right)$$

with

$$\Gamma_{E_3} = \Gamma^0 - \left(1 + \frac{[Q]_{x=0}}{K_{3,M}}\right)\Gamma_{E_2} - \left(1 + \frac{[S]_{x=0}}{K_{1,M}}\right)\Gamma_E \quad (10)$$

and, as initial conditions

$$\Gamma_E = 0,\ \Gamma_{E_2} = \Gamma^0\frac{k_6}{k_4C_S^0 + k_6},\ \Gamma_{E_3} = \Gamma^0\left(1 - \frac{k_6}{k_4C_S^0 + k_6}\right) \quad (11)$$

Any cyclic voltammogram may be simulated by numerical resolution of the above system of equations, introducing appropriate values for the all set of parameters as will be discussed later on. For the moment, we are looking for a simplified situation allowing a simpler derivation of the key-parameters from the experimental data. This can be obtained if the steady-state approximation applies for every enzyme form. Under such conditions (see the Supporting Information)

$$\frac{i_{cat}}{FS} = \frac{2k_3[Q]_{x=0}\Gamma^0}{1 + \frac{[Q]_{x=0}}{K_{3,M}} + \left(1 + \frac{[S]_{x=0}}{K_{1,M}}\right)\frac{k_3[Q]_{x=0}}{k_1[S]_{x=0}} + \frac{k_4[S]_{x=0}}{k_5[Q]_{x=0} + k_6}} \quad (12)$$

$[Q]_{x=0}$ being given by eq 3. According to the value of the substrate concentration various simplified versions of the steady-state response are applicable. For large enough H_2O_2 concentrations, its consumption is negligible and eq 12 may therefore be simplified into eq 13 by making $[S]_{x=0} = C_S^0$

$$\frac{i_{cat}}{FS} = \frac{2k_3[Q]_{x=0}\Gamma^0}{1 + \frac{[Q]_{x=0}}{K_{3,M}} + \left(1 + \frac{C_S^0}{K_{1,M}}\right)\frac{k_3[Q]_{x=0}}{k_1C_S^0} + \frac{k_4C_S^0}{k_5[Q]_{x=0} + k_6}} \quad (13)$$

A plateau-shaped curve, independent of scan rate, with superimposed forward and backward traces, is then expected. As seen in Figure 3, these features are found only for large H_2O_2 concentrations. In this range of substrate concentrations, eq 13 further simplifies, because reaction 1 is now so rapid that reaction 3 becomes the sole rate-determining step. Then, the plateau current ($i_{p,cat}$) is given by

$$\frac{i_{p,cat}}{FS} = \frac{2k_3C_P^0\Gamma^0}{1 + \frac{C_P^0}{K_{3,M}} + \frac{k_4C_S^0}{k_6 + k_5C_P^0}} \quad (14)$$

Experiments fulfilling these requirements were carried out with 2 and 10 mM H_2O_2 (Figure 5). They can be exploited to derive

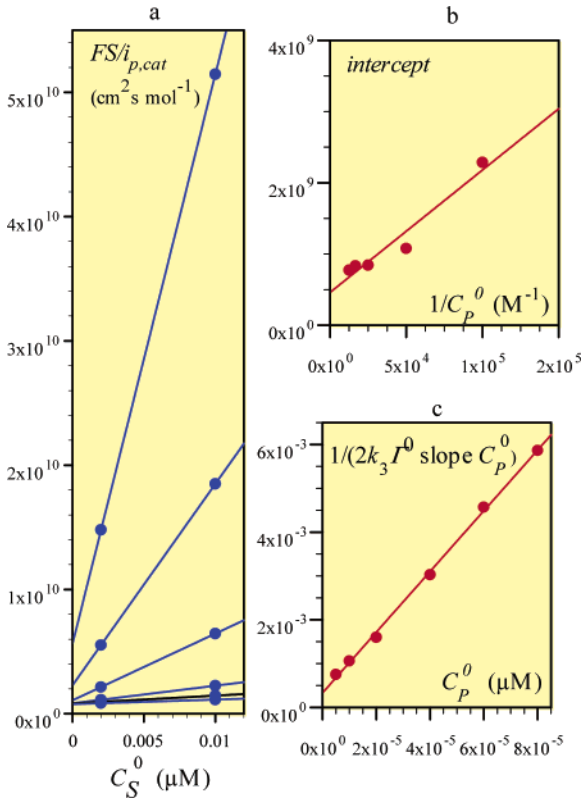

Figure 5. (a) Inverse of the catalytic plateau current obtained at the same IgG-b-coated SPE as in Figure 3 as a function of the substrate concentration for increasing values of the cosubstrate concentration (from top to bottom: 5, 10, 20, 40, 60, 80 μM) in PB. Scan rate: 10 mV s^{-1}. Temp.: 20 °C. (b) plot of the intercept in Figure 5a against the reciprocal of the cosubstrate concentration. (c) plot of the reciprocal of the slope in Figure 5a against the cosubstrate concentration.

the main parameters after recasting eq 14 as follows

$$\frac{FS}{i_{p,cat}} = \frac{1}{2k_3\Gamma^0}\left(\frac{1}{C_P^0} + \frac{1}{K_{3,M}}\right) + \frac{1}{2k_3\Gamma^0}\frac{C_S^0}{\frac{k_6}{k_4} + \frac{k_5}{k_4}C_P^0} \quad (15)$$

Plotting first the reciprocal of the catalytic plateau current against the substrate concentration (Figure 5a) and then the intercept of this plot against the reciprocal of the cosubstrate concentration (Figure 5b), allows the determination of $k_3\Gamma^0 = 0.029$ cm s^{-1} (slope) and $K_{3,M} = 37$ μM (intercept). Plotting next the reciprocal of the slopes of Figure 5a straight lines against the cosubstrate concentration (Figure 5c) allows the determination of $k_5/k_4 = 69.3$ (slope) and $k_6/k_4 = 3.3 \times 10^{-4}$ M^{-1} (intercept).

Using these values, we can see that the predictions of eq 14 concerning the variation of the plateau current with the substrate concentration (blue line in Figure 4) match the experimental data in the upper side of the substrate concentration range. One of the reasons that this equation ceases to represent correctly the phenomena upon decreasing the substrateconcentration is that reaction 1 interferes more and more in the rate control of the catalytic loop. Maintaining the steady-state approximation and assuming that the consumption of the substrate is negligible, we may thus try eq 13, taking literature values for the kinetics characteristic of reaction 1, $k_1 = 1.7 \times 10^7$ M^{-1} s^{-1} and $K_{1,M} = 128$ μM.[23] The ensuing red line in Figure 4 indeed exhibits a strong decrease as the substrate concentration decreases but

does not quite fit the experimental data. The reason for this lack of agreement is that we have neglected the consumption of the substrate, which should in fact start to interfere more and more as the substrate concentration decreases.

The gradient of S that is being established in the solution when it is consumed at the electrode surface may be depicted as follows, neglecting the amount of S consumed by reaction 4 in Scheme 1

$$D_S\left(\frac{\partial[\mathrm{S}]}{\partial x}\right)_{x=0} = k_1[\mathrm{S}]_{x=0}\Gamma_\mathrm{E} \tag{16}$$

Taking into account the boundary conditions, the time-dependent substrate concentration at $x=0$ is then given by the following convolution integral equation (see the Supporting Information)

$$\frac{[\mathrm{S}]_{x=0}}{C_S^0} = 1 - \frac{\sqrt{D_S}}{\sqrt{\pi}C_S^0}\int_0^t \left(\frac{\partial[\mathrm{S}]}{\partial x}\right)_{x=0}\frac{d\eta}{\sqrt{t-\eta}} = 1 - \frac{1}{\sqrt{\pi}\sqrt{D_S}}\int_0^t \frac{k_1\Gamma_\mathrm{E}[\mathrm{S}]_{x=0}}{C_S^0}\frac{d\eta}{\sqrt{t-\eta}} \tag{17}$$

Still keeping with the steady-state approximation, we may introduce the value of $[\mathrm{S}]_{x=0}$ deriving from the numerical resolution of eq 17 into eq 12. A simpler version, applicable at the lower end of the substrate concentration range, which emphasizes the role of substrate consumption, is when inactivation of the enzyme is neglected. Then eq 12 simplifies into eq 18

$$\frac{i_\mathrm{cat}}{FS} = \frac{2k_1\Gamma^0[\mathrm{S}]_{x=0}}{1 + [\mathrm{S}]_{x=0}\left[\frac{k_1}{k_3}\left(\frac{1}{[\mathrm{Q}]_{x=0}} + \frac{1}{K_{3,\mathrm{M}}}\right) + \frac{1}{k_1K_{1,M}}\right]} \tag{18}$$

The cyan curve in Figure 4 thus results from the combination of eq 18 with the numerical resolution of eq 17. It is seen to match satisfactorily the experimental data in the low substrate concentration range.

When complete control by substrate diffusion is reached, the current−potential response obeys the conditions of "total catalysis", being given by eq 19 (magenta curve in Figure 4), whereas the peak potential is given by eq 20[20]

$$i_\mathrm{p,cat} = 2 \times 0.609\mathrm{FSC}_S^0\sqrt{D_S}\sqrt{\frac{Fv}{RT}} \tag{19}$$

$$E_p = E^0_\mathrm{P/Q} + \frac{RT}{F}\ln\left(\frac{\Gamma^0k_3C_P^0}{C_S^0\sqrt{D_S}\sqrt{\frac{Fv}{RT}}}\right) \tag{20}$$

The last theoretical approach that we may envisage in the framework of the steady-state approximation consists of introducing the value of $[\mathrm{S}]_{x=0}$ deriving from the numerical resolution of eq 17 into eq 12. Thus, substrate consumption and diffusion would be taken care of together with inhibition. The result is the green curve in Figure 4, which fits the experimental data at low and high substrate concentrations. We may note in this connection that in the intermediate substrate concentration range

(23) Rodriguez-Lopez, J. N.; Gilabert, M. A.; Tudela, J.; Thorneley, R. N. F.; Garcia-Canovas, F. *Biochemistry* **2000**, *39*, 13 201.

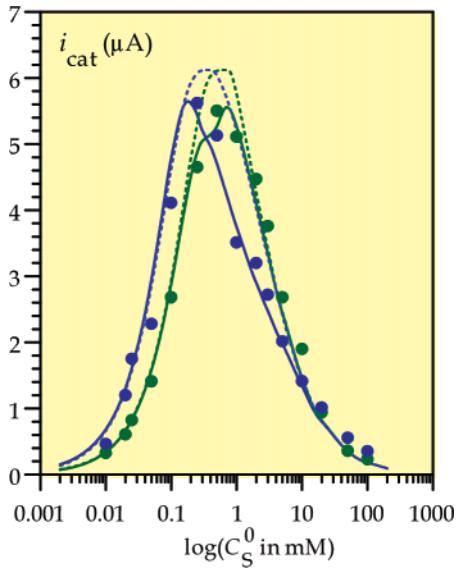

Figure 6. Same conditions as in Figures 3 and 4 except for the scan rate. Green and blue symbols and curves are for $v = 0.01$ and 0.05 V/s, respectively. Solid circles: experimental points. Dotted lines: application of equations (12) and (17), with: $k_3\Gamma^0 = 0.029$ cm s^{-1}, $K_{3,\mathrm{M}} = 37$ μM, $k_4/k_5 = 0.0144$, $k_6/k_5 = 4.8$ μM, $k_1 = 1.7 \times 10^7$ M^{-1} s^{-1}, $K_{1,\mathrm{M}} = 128$ μM, $D_\mathrm{S} = 1.5 \times 10^{-5}$ cm^2 s^{-1}. Full lines: simulation after removal of the steady-state approximation and using the same values of the preceding parameter plus $k_4 = 30$ M^{-1} s^{-1}.

(0.3 to 3 mM), the green curve overshoots the red curve, and adheres more closely to the experimental data. The reason is that substrate consumption was neglected in the construction of the red curve. In fact, substrate consumption decreases its concentration at the electrode surface, and consequently, the extent of inhibition, thus resulting in an enhancement of the catalytic current.

Although better with the green curve than with the red curve, the adherence to the experimental data is not complete in the intermediate concentration region. It is interesting to note in this connection that hysteresis and trace crossing appear in this concentration range, in line with the notion that reactions 4, 5, and 6 have then not enough time to reach steady state during the potential scan. This is confirmed by the observation that raising the scan rate entails a stronger divergence between the theoretical curve (Figure 6, dotted lines) and the experimental points.

Simulation of the experimental data within the intermediary zone of substrate concentration thus requires removing the steady-state approximation and compute the current potential curves by numerical resolution of eqs 7−11 (see the Supporting Information). For this, we start from the set of values obtained above for $k_3\Gamma^0$, $K_{3,\mathrm{M}}$, k_5/k_4, k_6/k_4, and use the time dependence of hysteresis to adjust the individual values of k_4, k_5, k_6. The result of the fitting is shown for individual current−potential responses in Figure 3 and for peak or plateau currents in Figures 4 and 6. The agreement between theory and experiment is excellent in all cases for the following values of $k_4 = 30$ M^{-1} s^{-1}, $k_5 = 2080$ M^{-1} s^{-1}, and $k_6 = 0.01$ s^{-1}.

Another aspect of the catalytic current responses concerns the variation of the peak potential at low H_2O_2 concentrations, when the current−potential responses are peak-shaped, being partially controlled by H_2O_2 diffusion. The peak potential is then expected to shift in the positive direction upon increasing

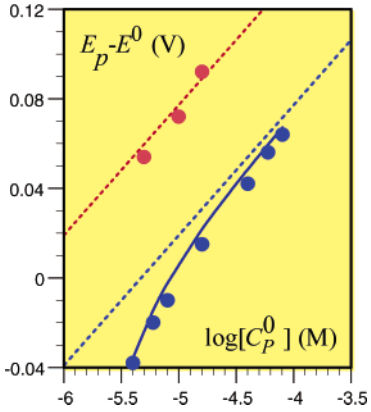

Figure 7. Same conditions as in Figures 3 and 4. Variation of the peak potential with the cosubstrate concentration for $[H_2O_2] = 5\ \mu M$ (red circles) and 50 μM (blue circles). Dotted lines: application of eq 20. The plain blue curve is obtained by full simulation for 50 μM H_2O_2 with $k_3\Gamma^0 = 0.029$ cm s^{-1}, $K_{3,M} = 37\ \mu M$, $k_4 = 30\ M^{-1}\ s^{-1}$, $k_5 = 2080\ M^{-1}\ s^{-1}$, $k_6 = 0.01\ s^{-1}$, $k_1 = 1.7 \times 10^7\ M^{-1}\ s^{-1}$, $K_{1,M} = 128\ \mu M$, $D_S = 1.5 \times 10^{-5}$ $cm^2\ s^{-1}$.

the cosubstrate concentration, control by substrate diffusion being reached at the lowest concentrations, in which case the variation of the peak potential with C_P^0 is depicted by eq 20. This is illustrated in Figure 7 for two different values of $[H_2O_2]$, where it is seen that the peak potential variations match satisfactorily the theoretical curve obtained by full simulation and the diffusion-controlled behavior for the lowest substrate concentration and/or higher cosubstrate concentration.

Determination of the Enzyme Coverage. Activity of the Immobilized Enzyme. The fact that the values of the rate constants k_4, k_5, and k_6 obtained in the preceding section (30 $M^{-1}\ s^{-1}$, 2080 $M^{-1}\ s^{-1}$, 0.01 s^{-1}, respectively) are close to those characterizing the enzyme in solution (55 $M^{-1}\ s^{-1}$, 1900 $M^{-1}\ s^{-1}$, 0.012 s^{-1}, respectively)[15] is a first indication that the enzyme approximately preserved all of its activity upon immobilization. Pointing to the same conclusion is the observation that the value of $K_{3,M}$ found here (37 $\pm$ 15 μM) is consistent with the value in solution (25 $\pm$ 10 μM), although the uncertainty is rather large in both cases. May we come to the same conclusion for what concerns the main catalytic loop? Namely, is the enzyme activity preserved at the level of rate constant k_3, is the question we address now. As an outcome of the analysis developed in the previous section, we found that $k_3\Gamma^0$ is equal to 0.029 cm s^{-1}, with no indication of the values of the two independent parameters k_3 and Γ^0. If it were assumed that the value of k_3 is the same as in solution ($7.85 \times 10^6\ M^{-1}\ s^{-1}$) the value of Γ^0 would be $\Gamma_e^0 = 3.7$ pmol cm^{-2}. If the actual value of Γ^0, Γ_t^0, is known independently, the degree of activity of the immobilized enzyme may then be obtained as the ratio $\alpha = \Gamma_e^0/\Gamma_t^0$, which measures the extent to which the activity is preserved upon immobilization. This approach of enzyme activity implies that over Γ_t^0 moles of enzyme on the electrode surface, Γ_e^0 moles are fully active whereas $\Gamma_t^0 - \Gamma_e^0$ moles are fully inactive. Another conception of enzyme activity is to view the activity of all of the Γ_t^0 enzyme molecules on the surface diminished to the same extent. Then the common rate constant is $k_3^{im} = (k_3\Gamma^0)/\Gamma_t^0$ and the degree of activity is the ratio of the immobilized over homogeneous enzyme rate constant, $\alpha = k_3^{im}/k_3^{hom}$. The result is the same in both cases. Kinetic approaches such as the one developed here are indeed not able to distinguish between the two possibilities.

One possible access to Γ_t^0, is to "weight" the mass of a HRP monolayer deposited on a gold surface with a *quartz crystal microbalance*.[10a,11a,b,24] However, the method suffers from a serious source of uncertainty. The frequency of the quartz crystal resonators is indeed sensitive to the density, roughness, and viscoelasticity of the biofilm,[25] rendering its correlation with the change in mass at the device-liquid interface particularly difficult, as recently demonstrated for the adsorption of biotin conjugate-avidin complexes to the gold electrode of a quartz crystal microbalance.[25a] *Spectrophotometric* methods taking advantage of the high absorption coefficients of the heme group contained in HRP[11f] or of a *fluorescent probe* coupled to HRP,[12b,13b] have also been employed for the estimation of the surface coverage of monolayer or multilayers of HRP immobilized on quartz plates. However, these latter methods are restricted to UV-transparent supports and, in the case of a fluorescence measurement, the probe can be quenched by the environment of the solid surface. *Radioactive labeling* was proved to be a more efficient strategy for the precise determination of the coverage of a protein specifically attached on a carbon electrode.[14e] However, owing to the delicate handling of radioactive reagents, the use of the method for a systematic control of the surface concentration is not very convenient.

Before coming to our proposal of a simpler approach, namely the *droplet depletion method*, a comment on the widely used *colorimetric detection technique*[7b−f,10c,11b,12,13a,b,24a] seems worthwhile. The method is often presented as giving an access to the total surface concentration of the immobilized enzyme. In fact, it does not, as results from the following reasons. The immobilized HRP is immersed in a spectrophotometric cuvette containing a stirred solution of a chromogenic cosubstrate and H_2O_2 (the concentrations are usually sufficiently large for the steady-state conditions to apply) for a fixed incubation period, followed by the adsorption measurement of the enzyme generated product released in the bulk volume of the solution. The enzyme coverage of active HRP is then drawn from comparison with the optical densities of known concentrations of soluble HRP obtained under the same conditions. The validity of the method hinges upon two assumptions. One is that the immobilized enzyme has the same activity as the soluble enzyme. The other is that that the substrate and cosubstrate mass-transfer limitations do not interfere in the catalytic efficiency of the immobilized enzyme. That these requirements are not actually fulfilled in most cases results from the following observations. With the same immobilized system as in the preceding electrochemical experiments, we have used the colorimetric method with 3,5,3′,5′-tetramethylbenzidine, as chromogenic reagent, and found an average value of $\Gamma^0 = 0.12 \pm 0.03$ pmol cm^{-2} for a series of 3 electrodes coated with a monolayer of IgG-b/N−HRP, assuming that all enzyme molecules on the surface are fully active. This value is 32 times lower than the average value of $\Gamma_e^0 = 3.8 \pm 1.1$ pmol cm^{-2} derived from the above electrochemical experiments with the same system, under the same assumption. The much lower value of enzyme coverage

(24) (a) Berzina, T. S.; Piras, L.; Troitsky, V. I. *Thin Solid Films* **1998**, *327−329*, 621. (b) Tatsuma, T.; Ariyama, K.; Oyama, N. *J. Electroanal. Chem.* **1998**, *446*, 205.
(25) (a) Ghafouri, S.; Thompson, M. *Langmuir* **1999**, *15*, 564. (b) Buttry, D. A.; Ward, M. D. *Chem. Rev.* **1992**, *92*, 1355.

obtained with the spectrophotometric experiment strongly suggest a mass transfer limitation at the electrode surface, leading to a considerable underestimation of the activity of the immobilized enzyme. In fact, a reliable use of the colorimetric method would require that the kinetic and mass transport factors be deciphered along the same lines as in the above analysis of the electrochemical responses. Such an analysis would yield the product ($k_3\Gamma^0$), the dissection of which would require the same independent determination of Γ_t^0 as it does in the electrochemical case.

The *droplet depletion method* for determining Γ_t^0 consists of depositing a droplet of N−HRP solution on the surface of the IgG-b-coated electrode and determining spectrophotometrically, after an incubation period, the remaining activity of the enzyme contained in the droplet. On account of the large ratio of electrode surface/droplet volume, a sizable amount of dissolved N−HRP is depleted from the drop. This amount of enzyme normalized toward the surface area of the electrode, which we call Γ_{depl}^0, corresponds in principle to the amount specifically attached to the electrode surface, Γ_t^0 that we are hunting for. However, the following difficulties appear. In the first experiments, carried out with drops simply prepared by dilution of a stock solution of N−HRP with a phosphate buffer (pH 7.4), the average surface concentration of active enzyme at the surface of IgG-b-coated SPEs was found to be absurdly large ($\Gamma_t^0 = \Gamma_{depl}^0 = 11.8$ pmol cm^{-2}) as compared with a rough estimate based on protein sizes (3.3 pmol cm^{-2} for a saturated monolayer)[26] and to the value derived from the voltammetric responses under the assumption of that the immobilized enzyme is fully active ($\Gamma_e^0 = 3.8$ pmol cm^{-2}). The suspicion that the results may be due to the real surface area of the SPE being larger than its geometric surface area was lifted when similar results were obtained at a highly oriented pyrolytic graphite electrode which real and geometric area are practically the same (all the data are summarized in Table 1). These results points to the "disappearance" of a substantial amount of the enzyme besides the quantity that has been specifically attached to the electrode surface. This supposition was confirmed by an experiment in which the first layer of IgG-b was replaced by a layer of nonspecific protein like bovine serum albumin (BSA), an abnormally high nonspecific surface concentration of N−HRP ($\Gamma_{depl;NS}^0$) was obtained under the same conditions, whereas the catalytic current in cyclic voltammetry was close to zero.[27] This observation suggests that, during the incubation time, a significant amount of the enzyme is inactivated, probably denatured at the air−water interface, the ratio surface area/volume being particularly large in the drop configuration.[28] Addition of BSA to the solution[29] entails a decrease of the loss of enzyme, the values of the enzyme coverage, determined by droplet depletion method being then closer to the values obtained by cyclic voltammetry on both types of electrodes (Table 1). The problem is however not completely eliminated as revealed by the fact that, in the absence of IgG-b coating and presence of BSA, depletion of N−HRP still occurs (Table 1), albeit to a much lesser extent than in the absence of BSA ($\Gamma_{depl;NS}^0 \sim 1.5$ pmol cm^{-2}). We may use this observation to correct the estimation of Γ_t^0 (i.e., $\Gamma_{depl,cor}^0$). The results are given in Table 1, indicating that $\sim(75 \pm 30)$% of the immobilized enzyme on the electrode remains fully active, on both electrodes.

Table 1. Estimation of the Surface Concentrations (in pmol cm^{-2}) of N−HRP Specifically Immobilized at IgG-b-Coated Electrodes

electrode	SPE		HOPG	
solution[a]	PB[b]	PB + 0.1% BSA	PB	PB + 0.1% BSA
Γ_{depl}^0[c]	11.8 ± 0.3	7.2 ± 0.8	11.0	6.7 ± 0.1
$\Gamma_{depl,NS}^0$[d]	5.8 ± 3	1.5 ± 0.6	5.5	1.5 ± 0.7
$\Gamma_{depl,cor}^0$[e]	6 ± 3	5.7 ± 1.0	5.5	5.2 ± 0.70
Γ_e^0[f]	3.8 ± 0.5	3.9 ± 1.0	4.6	3.9 ± 1.0
$\Gamma_{e,NS}^0$[g]	~0.026	~0	0.25	0
$\Gamma_{depl}^0/\Gamma_e^0$	3.1	1.7	2.4	1.7
α[h]	0.63 ± 0.5	0.72 ± 0.26	0.84	0.75 ± 0.30

[a] Bulk concentration of N−HRP: 0.2 μM. [b] Phosphate buffer. [c] Surface concentration of N−HRP from the droplet depletion method at a IgG-b-coated electrode. [d] Surface concentration of N−HRP from the droplet depletion method in the absence of IgG-b-coating. [e] $\Gamma_{depl,cor}^0 = \Gamma_{depl}^0 - \Gamma_{depl,NS}^0$. [f] Surface concentration of N−HRP from the cyclic voltammetric catalytic current at a IgG-b-coated electrode. [g] Surface concentration of N−HRP from the cyclic voltammetric catalytic current in the absence of IgG-b-coating. [h] Degree of activity of the immobilized enzyme $\alpha = \Gamma_e^0/\Gamma_t^0 = \Gamma_e^0/\Gamma_{depl,cor}^0$.

Analytical Sensitivity of the Enzyme Electrode. Because one of the objectives of HRP-based electrodes is the determination of minute concentrations of H_2O_2, it is worth evaluating its analytical performances in terms of sensitivity, detection limit and extent of the linear range of the calibration curve. The present work shows that a single monolayer of HRP is largely sufficient to reach the maximal sensitivity of H_2O_2 detection and that there is no advantage increasing the deposited amount of HRP, except for an extension of the linear range of the calibration curve. Using a diffusion coefficient of H_2O_2 equal to 1.5×10^{-5} cm^2 s^{-1} (see the Experimental section), eq 19 allows one to calculate a maximal sensitivity of $i_p/SC_S^0 = 0.47$ A M^{-1} cm^{-2} at, e.g., $\upsilon = 10$ mV s^{-1} or $i_p/SC_S^0 = 1.05$ A M^{-1} cm^{-2} at, e.g., $\upsilon = 50$ mV s^{-1}. These theoretical sensitivities are close to the experimental values obtained at the lowest H_2O_2 concentrations, i.e., 0.35 A M^{-1} cm^{-2} at 10 mV and 0.88 A M^{-1} cm^{-2} at 50 mV s^{-1}, confirming that we are not far then from total catalysis, and therefore, complete control by mass transport of H_2O_2. It is worth noting that a higher sensitivity can be obtained by increasing the scan rate. The increase of sensitivity with the scan rate is analogous to the increase of the

(26) The crystallographic X-ray studies have given protein sizes of ~4.0 × 3.5 × 6.0 nm and of 4.0 × 5.5 × 5.5 nm for the HRP[26a] and avidine,[26b] respectively. Taking into account that each HRP is coupled to one molecule of neutravidin[26c] and that the conjugate may be attached perpendicularly on the biotinylated electrode surface through its neutravidin function, a projection area of ~30 nm^2 can be calculated. Because the binding on the surface occurs randomly, the maximum of the electrode coverage should be 60% of the area.[26d] Thus each molecule of HRP should occupy an area of ~50 nm^2 and the maximal surface concentration, which should correspond to the saturation of a monolayer on a perfectly flat surface, can be estimated as 3.3×10^{-12} mol cm^{-2}. (a) Henriksen, A.; Smith, A. T.; Gajhede, M. *J. Biol. Chem.* **1999**, *274*, 35 005. (b) Pugliese, L.; Coda, A.; Malcovati, M.; Bolognesi, M. *J. Mol. Biol.* **1993**, *231*, 698. (c) The dimensions of neutravidin are probably slightly lower than those of avidin, because it is a deglycosylated form of avidin and its molecular weight (MW = 60 000) is somewhat lower than avidin (MW = 67 000). (d) Finegold, L.; Donnel, J. T. *Nature* **1979**, *278*, 153.

(27) The presence of 0.1% BSA in the phosphate buffer used all along the immobilization procedure has the further beneficial effect to significantly reduce the nonspecific catalytic current as illustrated in Table 1.

(28) (a) The HRP denaturation at the air−water interface as been suspected during the preparation of an HRP monolayer by the Langmuir−Blodgett technique.[28b] (b) Berzina, T. S.; Piras, L.; Troitsky, V. I. *Thin Solid Films* **1998**, *327*, 621.

(29) (a) The bovine serum albumin has been shown to stabilized highly diluted solutions of HRP-conjugates, probably by minimizing their loss by adsorption on the wall of the container.[29b] (b) Eremin, A. N.; Budnikova, L. P.; Sviridov, O. V.; Metelitsa, D. I. *Applied Biochem. Microbiol.* **2002**, *38*, 151.

rotation rate of a rotating disk electrode, i.e., RT/Fv in eq 19 is replaced by δ^2/D_S in rotating disk experiments (δ is the thickness of the diffusion layer in centimeters). For example, maximal sensitivities of ca. 1 A M^{-1} cm^{-2} have been previously obtained for the amperometric reduction of H_2O_2 at a rotating disk electrode (1000 rpm) modified with a thin layer of HRP embedded in a poly(4-vinylpyridine) based redox hydrogel having $[Os(bpy)_2pyCl]^{3+/2+}$ redox centers.[8c]

The detection limit can be estimated from the lowest catalytic current that might be discernible after subtraction of the reversible wave of the mediator obtained in the absence of H_2O_2. Considering that 2 nA of background noise measured at 10 mV s^{-1} is equivalent to a 6×10^{-8} M H_2O_2, a detection limit of 2×10^{-7} M H_2O_2 can be estimated assuming a signal-to-noise ratio of 3.

Amperometric immunosensors or DNA-sensing devices are other important applications of HRP-based electrodes. HRP is then used as an amplifying label to sense the specific biomolecular recognition occurring at the electrode surface between an antigen and an antibody[17] or between a DNA target and a DNA probe.[18] The analytical performances of the device are then closely related to its capacity to detect low surface concentrations of the enzyme label specifically anchored on the electrode surface. The choice of the substrate and cosubstrate concentrations, as well as the scan rate, are then of crucial importance. From the bell-shaped curves in Figure 4, it appears that, at a given scan rate, the catalytic current is maximal for an optimal concentration of H_2O_2. If we consider the scan rate of 10 mV s^{-1}, then the maximal sensitivity is reached for ~0.5 mM H_2O_2, which corresponds to a current density of ~55 μA cm^{-2}. Because the catalytic current is a linear function of the enzyme coverage (eq 12), the lowest detectable surface concentration of HRP would have to be limited by the noise of the background current. Considering a background noise of 0.02 μA cm^{-2} at 10 mV s^{-1} and the absence of nonspecific binding, a detection limit of $\Gamma^0 = 4 \times 10^{-15}$ mol cm^{-2} can be estimated, assuming a signal noise ratio of 3.

Concluding Remarks

After examination and testing of several strategies, the use of a sacrificial biotinylated immunoglobulin for rapid biotinylation of the electrode surface followed by the anchoring of an avidin-enzyme conjugate appears as a particularly simple and efficient procedure for depositing an HRP monolayer onto an electrode surface. It allows a high-yield immobilization of the enzyme leading to a stable and highly catalytic coating.

Cyclic voltammetry is a convenient means for analyzing the catalytic reduction of H_2O_2 at such HRP monolayer electrodes in the presence of $[Os^{III}(bpy)_2pyCl]^{2+}$ as a one-electron reversible cosubstrate. The odd shapes of current−potential responses, unusual bell-shaped variation of the peak or plateau current with the substrate concentration, hysteresis and trace crossing phenomena, dependence or lack of dependence with the scan rate, can all be explained and quantitatively analyzed in the framework of the catalysis/inhibition mechanism depicted in Scheme 1, taking mass transport of substrate and cosubstrate into account. According to H_2O_2 concentration, limiting-behavior analyses based on the dominant factors or complete numerical simulation were used in the treatment of experimental data. The kinetic characteristics derived from these quantitative treatments implemented by the determination of the amount of enzyme deposited by the newly developed droplet depletion method allowed a comparison with homogeneous characteristics to be drawn. It shows that HRP remains nearly fully active once anchored on the electrode surface through the avidin−biotin linkage.

Although not very accurate (relative standard deviation of ~30%), the droplet depletion method is, with the possible exception of the burdensome radioactive labeling technique, the most reliable among the available methods for the determination of the enzyme coverage.

Among the various electrochemical techniques used for the determination of H_2O_2 at a HRP-based enzyme electrode, amperometry at controlled potential is the most employed.[8,9b,10,11d,f−h] Besides the advantage of simplicity, the method has the drawback that it cannot discriminate between a high or a low H_2O_2 concentration, depending if we are on the left or on the right of the bell-shaped calibration curve. The doubt can of course be eliminated by sample dilution, but this is at the expense of the simplicity of the procedure. In cyclic voltammetry, this ambiguity does not exist, since a simple examination of the shape of the catalytic wave allows knowing in which part of the bell-shaped calibration curve we are (i.e., at high substrate concentration the forward current is lower than the reverse one and, at low concentration the catalytic wave is peak-shaped).

Experimental Section

Reagents. Lyophilized HRP (mainly composed of isoenzyme C) was purchased from Sigma (type VI; RZ = 3.1). Lyophilized biotinylated rabbit IgG (immunopure, whole molecule) and lyophilized neutravidin HRP conjugate were obtained from Pierce and they were used without further purification. The concentrations of HRP or N−HRP were determined spectrophotometrically using the Soret extinction coefficient of 102 mM^{-1} cm^{-1} at 403 nm. The chromogenic cosubstrate 3,5,3′,5′-tetramethylbenzidine was supplied by Aldrich. The $[Os^{II}(bpy)_2pyCl]$-PF_6 was synthesized as previously described.[30] Its oxidized form, ($[Os^{III}(bpy)_2pyCl](PF_6)_2$), was obtained by chemical oxidation with $AgPF_6$ (from Aldrich). Hydrogen peroxide (50%) was supplied by Prolabo (reagent-grade product). Its concentration was determined by permanganate titration. The phosphate buffer (PB, 4.3 mM NaH_2PO_4, 15.1 mM Na_2HPO_4, and 50 mM NaCl, pH 7.4, leading to an ionic strength of 0.1 M) and all of the other aqueous solutions were prepared using water purified by a Milli-Q water purification system from Millipore. Polypropylene containers were used to minimize HRP loss from solution.

Steady-State Kinetics of the Reaction of N−HRP with Os^{II}. A Hewlett-Packard 8452 diode array spectrophotometer interfaced with a PC computer was used for UV−visible absorbance measurements. Steady-state kinetics were studied as previously[15] by following at 500 nm ($\epsilon_{500\ nm}$ = 8.7 mM^{-1} cm^{-1}) the initial rates of $[Os^{II}(bpy)_2pyCl]^+$ oxidation at 20 °C as a function of the reducing substrate concentration. The reactions were initiated by addition of H_2O_2 (final concentration of 0.1 mM) to a mixture of HRP (0.2 nM) and $[Os(bpy)_2pyCl]^+$ (ranging from 0.2 μM to 0.15 mM) in PB. The reciprocal plot of the dependence of the initial rate on the initial concentration of Q was fitted to the eq 4 in ref 18 and the values of k_3 and $k_{3,2}$ were calculated considering that the values of $k_1 = 1.7 \times 10^7$ M^{-1} s^{-1} and $k_{1,2} = 2170$ s^{-1} determined for the native HRP[23] remains unchanged for the N−HRP conjugate.

Electrochemical Experiments. An EG&G PAR potentiostat interfaced with a PC computer was used for the cyclic voltammetric

(30) Kober, E. M.; Caspar, J. V.; Sullivan, B. P.; Meyer, T. J. *Inorg. Chem.* **1988**, *27*, 4587.

experiments. Carbon-based screen-printed electrodes (SPE) of 9.6 mm^2 surface area for the sensing disk, were used as disposable working electrodes. They were prepared from a homemade carbon-based ink composed of graphite particles (Ultra Carbon, UCP 1M, Johnson Matthey) and polystyrene.[31] In a few experiments, the working electrode was a highly oriented pyrolytic graphite (HOPG) plate with an electroactive surface freshly cleaved by means of an adhesive tape and delimited by an insulating circular self-adhesive eyelet (5-mm-diameter, i.e., 0.2 cm^2) to form a small-volume electrochemical cell. Under these conditions, droplets of 30−50 μL can be deposited without being spread out. A saturated calomel electrode (SCE) was employed as reference electrode. The counter electrode was a platinum wire. With the exception of those performed with HOPG electrodes, which were performed at room temperature, the voltammetric experiments were done in a water-jacketed electrochemical cell maintained at 20 ± 0.5 °C with a circulating water bath. The diffusion coefficient of H_2O_2 was taken equal to 1.5×10^{-5} cm^2 s^{-1}.[32]

Immobilization Procedures. All experiments were performed at room temperature. A drop of 8 μL of 0.5 mg/mL IgG-b in PB was locally deposited on the sensing area of the SPE and incubated for 2 h in a water-saturated atmosphere. The electrode surface was then thoroughly rinsed with PB and dipped for 30 min in 2 mL of PB containing 0.1% BSA. After another thoroughly washing with PB, the specific recognition of N−HRP by the adsorbed IgG-b was performed by immersing the electrode in 2 mL of 20 μg/mL (i.e., 0.2 μM) of N−HRP diluted in PB for 2 h. In preliminary experiments, the concentration of N−HRP and the immersion time were varied so as to find optimal conditions to obtain a saturated monolayer of N−HRP. Finally, the enzyme electrode was rinsed and stored in PB at 4 °C until used. The nonspecific binding was obtained using the same procedure, except that the 8 μL of IgG-b first deposited were replaced by 8 μL of 0.1% BSA in PB.

Determination of the Enzyme Coverage from the Depletion of the N−HRP Contained in a Droplet Deposited on a SPE or HOPG Electrode. Drops of 8 μL or 35 μL containing 0.5 mg/mL IgG-b 0.1% BSA in PB were deposited on the active surface of a series of SPEs or HOPG electrodes, respectively, and incubated for 2 h in a water-saturated atmosphere. The electrodes were then rinsed with PB and dipped for 30 min in 2 mL of PB containing 0.1% BSA. After another washing with PB, drops of 5 μL or 15 μL of 20 μg/mL N−HRP in PB containing 0.1% BSA (in some experiments, a phosphate buffer without BSA was used as a dilution buffer, all along the procedure, see Table 1) were deposited on the surface of SPEs or HOPG electrodes, respectively, and then further incubated for 2 h in a water-saturated atmosphere. Next, each of the droplets deposited on the electrodes surfaces were transferred in vials filled with PB containing 0.1% BSA. In the case of the SPEs, the transfer of the droplet was simply accomplished by immersing the electrode in 4 mL of the buffer during 5−10 min, whereas in the case of the HOPG electrodes, the 15-μL drop was collected with a pipet and transferred into 3.785 mL of buffer, completed by 4 × 50 μL of buffer which have been used to carefully washed the HOPG surface. In parallel, reference solutions of N−HRP were prepared by diluting 5 μL or 15-μL of the 20 μg/mL N−HRP in a total volume of 4 mL of PB containing 0.1% BSA.

The activities of N−HRP contained in the 4 mL of vials were then determined spectrophotometrically as follows. To 2.4 mL of citrate buffer (0.1 M, pH 5.0), were added in order 50 μL of the diluted solution of N−HRP, 25 μL of 0.1 M of 3,5,3′,5′-tetramethylbenzidine in DMSO and 25 μL of 0.1 M H_2O_2 in PB. After thorough mixing and an incubation period of 10 min, the reaction was stopped by the addition of 1 mL of 1 N H_2SO_4. By lowering the pH-value, the enzyme generated blue radical cation of 3,5,3′,5′-tetramethylbenzidine is converted to a yellow diphenoquinoimine with a maximum extinction coefficient located at 450 nm.[33] The amount of N−HRP immobilized on the electrode was then indirectly determined from the decrease of N−HRP activity (i.e., decrease of absorbance) within the drop deposited on the electrode in comparison with the initial activity contained within the drop taken from the reference solution of N−HRP.

Spectrophotometric Determination of the Amount of Active Enzyme Immobilized on a SPE. A IgG-b/N−HRP modified SPE was immersed in a vial containing 2.45 mL of citrate buffer (0.1 M, pH 5.0), 25 μL of 0.1 M of 3,5,3′,5′-tetramethylbenzidine in DMSO and 25 μL of 0.1 M H_2O_2 in PB. After an incubation period of 8 min under stirring at room temperature, the electrode was removed and the solution acidified with 1 mL of 1 N H_2SO_4. The optical density was then recorded at 450 nm and compared with the optical densities of standard concentrations of soluble N−HRP (ranging from 1 to 5 pmole/L) obtained under the same conditions. From this comparison, the surface coverage of N−HRP was calculated.

Supporting Information Available: Derivation of eqs 3, 5, 8, 9, 12, 17 and numerical resolution of eqs 7−11 in the general case. This material is available free of charge via the Internet at http://pubs.acs.org.

JA0354263

(31) Bagel, O.; Limoges, B.; Schöllhorn, B.; Degrand, C. *Anal. Chem.* **1997**, *69*, 4688.
(32) Prabhu, V. G.; Zarapkar, L. R.; Dhaneshwar, R. G. *Electrochim. Acta* **1981**, *26*, 725.
(33) Porstmann, B.; Porstmann, T. In *Non Isotopic Immunoassay*; Ngo, T. T., Ed.; Plenum Press: New York, 1988; pp 57−84.